

# Distributionally Robust Statistical Verification with Imprecise Neural Networks

Souradeep Dutta<sup>1</sup>

Michele Caprio<sup>1</sup>

Vivian Lin<sup>1</sup>

Matthew Cleaveland<sup>1</sup>

Kuk Jin Jang<sup>1</sup>

Ivan Ruchkin<sup>2</sup>

Oleg Sokolsky<sup>1</sup>

Insup Lee<sup>1</sup>

*University of Pennsylvania<sup>1</sup>, University of Florida<sup>2</sup>*

DUTTASO@SEAS.UPENN.EDU

CAPRIO@SEAS.UPENN.EDU

VILIN@SEAS.UPENN.EDU

MCLEAV@SEAS.UPENN.EDU

JANGKJ@SEAS.UPENN.EDU

IRUCHKIN@ECE.UFL.EDU

SOKOLSKY@SEAS.UPENN.EDU

LEE@SEAS.UPENN.EDU

## Abstract

A particularly challenging problem in AI safety is providing guarantees on the behavior of high-dimensional autonomous systems. Verification approaches centered around reachability analysis fail to scale, and purely statistical approaches are constrained by the distributional assumptions about the sampling process. Instead, we pose a distributionally robust version of the statistical verification problem for black-box systems, where our performance guarantees hold over a large family of distributions. This paper proposes a novel approach based on a combination of active learning, uncertainty quantification, and neural network verification. A central piece of our approach is an ensemble technique called Imprecise Neural Networks, which provides the uncertainty to guide active learning. The active learning uses an exhaustive neural-network verification tool Sherlock to collect samples. An evaluation on multiple physical simulators in the openAI gym Mujoco environments with reinforcement-learned controllers demonstrates that our approach can provide useful and scalable guarantees for high-dimensional systems.

**Keywords:** statistical verification, reinforcement learning, imprecise probabilities, neural network verification.

## 1. Introduction

A major problem in analyzing safety for learning based autonomous systems is providing guarantees on the behavior ( Seshia et al. (2022); Divband Soorati et al. (2022)). The desirable behaviors can be on safety (“an undesired event will not happen”), liveness (“a desired event will eventually happen”), average performance (“the mean outcome is acceptable”), or generalized rewards (Song et al., 2022; Mitra, 2021). The quality of such behaviors can often be quantified with a scalar performance metric - quantitative semantics of STL, or rewards in an RL setting. In this paper our aim is to provide statistical estimates of this metric.

While model-based formal verification can give exhaustive guarantees on low-dimensional systems, high-dimensional ones are practically analyzed with black-box statistical approaches (Corso et al., 2022; Zarei et al., 2020; Lew et al., 2022). Such approaches derive confidence-based guarantees from a finite sample of trajectories. Active learning with Gaussian Processes (GPs) can make sampling more efficient by guiding it toward higher-uncertainty regions of initial states (e.g., the location where an autonomous car starts a scenario) and dynamics parameters (e.g., the maximum

braking power). However, existing approaches to statistical verification give guarantees with respect to a *single, fixed distribution* of initial states or system parameters (often implicitly so) (Qin et al., 2021). As it is difficult to predict or impose an exact distribution of states/parameters, the up-front statistical guarantees may be disrupted by the distribution shift of real-world deployments (Sinha et al., 2022). Furthermore, uncertainty quantification with GPs of realistic autonomous systems with higher (10+) dimensions, has limited scalability and sample efficiency (Liu et al., 2020). This limits utility of GPs in high-dimensional settings.

This paper proposes an approach to distributionally robust statistical verification, with active learning for improved scalability. Instead of assuming a fixed distribution of initial states, we pose the problem of finding a *family of distributions* that can uphold an expected lower bound on the desired performance metric given a specified level of confidence. The resulting family describes a variety of deployment scenarios where our performance guarantee applies and, therefore, can be used as part of pre-deployment validation and online monitoring.

At the heart of our approach is a surrogate performance model of a black-box autonomous system implemented with a novel ensemble technique called *Imprecise Neural Network* (INN) (Oala et al., 2020; Caprio et al., 2022). The uncertainty measure provided by the INN guides the sampling process, which alternates with scalable re-training of the INN. We pair the INN with a neural-network verification tool SHERLOCK (Dutta et al., 2019b, 2018a) to obtain distributional guarantees within a neighborhood of the sampled points.

We evaluate our approach on 10 case studies of physics simulators (Mujoco, OpenAI Gym (Brockman et al., 2016)) with neural-network perception and control. The experiments show that our uncertainty quantification scales well to higher dimensions, and our approach is more robust to distribution shift than the baseline of conformal prediction.

This paper makes four contributions: 1. A novel formulation of distributionally robust statistical verification that enables a combination of statistical and exhaustive guarantees. 2. A scalable active learning algorithm that combines imprecise neural networks with formal verification. 3. A theoretical guarantee on the system’s worst-case performance for any distribution in a produced family. This allows us to extend our guarantees outside of the training distribution. 4. An experimental evaluation on a variety of autonomy benchmarks from OpenAI gymnasium.

## 2. Problem and Approach

### 2.1. Problem Formulation

Consider an autonomous system  $x_{t+1} \sim F(x_t)$ , where  $x \in \mathbb{R}^n$  and  $F$  is a stochastic vector-valued function that dictates the evolution of the system over time. In practice,  $F$  captures the composition of system dynamics with the control policy, and  $x$  belongs to a closed and compact set  $\mathcal{X}$ . Starting from some initial state  $x_0$ , and executing the closed-loop system for  $T$  steps generates a trajectory  $\tau_{x_0} := [x_0, x_1, \dots, x_T]$ , such that  $x_{i+1} \sim F(x_i)$ . Additionally, the real-valued random *performance variable*  $\psi$  assigns a scalar value to the trajectory  $\tau_{x_0}$ , and is thus dependent on  $x_0$ . It quantifies the performance or the degree of satisfaction of a desired property by trajectory  $\tau_{x_0}$ . Our goal is to obtain some performance guarantees when the initial value  $x_0$  is drawn from set  $\mathcal{X}_0 \subseteq \mathcal{X}$ . The set  $\mathcal{X}_0$  can be part of a high-dimensional space, rendering it computationally prohibitive to sample densely. Now, we expect  $x_0$  to be drawn according to some to-be-discovered set of distributions over this initial set  $\mathcal{X}_0$ . Our goal will be to lower-bound the chance of performance function  $\psi$  exceeding some threshold  $\epsilon$  for any distribution in the above set. We formalize this problem below:

**Problem:** Consider a set of initial states  $\mathcal{X}_0$ , a performance function  $\psi$ , and a confidence parameter  $\lambda > 0$ . Let  $A = \{\psi(x_0) \geq \epsilon\}$ , for some performance threshold  $\epsilon > 0$ . We want to find an  $\epsilon$  and a family of distributions  $\mathcal{P}$  over the space  $\mathcal{X}_0 \times \mathbb{R}$  of initial states and performances, such that — in expectation — the conditional probability of event  $A$  when sampling initial states  $x_0$  from any distribution in  $\mathcal{P}_{\mathcal{X}_0}$  is at least  $(1 - \frac{1}{\lambda})$ . Here,  $\mathcal{P}_{\mathcal{X}_0}$  is the set of marginals of the elements of  $\mathcal{P}$  over  $\mathcal{X}_0$ . Mathematically, this means that

$$\mathbb{E}_{X \sim P_{\mathcal{X}_0}} [P_{\psi(x_0)|X=x_0}(\psi(x_0) \geq \epsilon)] \geq \left(1 - \frac{1}{\lambda}\right) \quad (1)$$

for all  $P_{\mathcal{X}_0} \in \mathcal{P}_{\mathcal{X}_0}$  and all conditional probabilities  $P_{\psi(x_0)|X=x_0}$ .

To elaborate further, the term  $P_{\psi(x_0)|X=x_0}(\psi(x_0) \geq \epsilon)$  captures the probability that the system’s performance is above some threshold  $\epsilon$ , under the stochasticity of the system’s evolution function  $F$ . An additional challenge lies in the fact it must hold over a family of distributions  $\mathcal{P}_{\mathcal{X}_0}$ . The expectation computes the fraction of samples expected to satisfy event  $A$  when the  $x_0$ ’s are drawn from the distribution  $P_{\mathcal{X}_0}$ . The inequality requires the expectation is above a threshold of  $(1 - \frac{1}{\lambda})$ . Note that from a practical standpoint we obtain meaningful bounds only for values of  $\lambda > 1$ .

## 2.2. Overall Approach

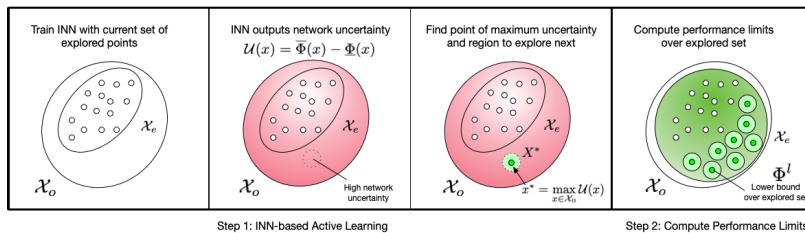


Figure 1: Here  $\mathcal{X}_0$  is explored across several iterations by employing an active learning strategy based on Imprecise Neural Networks (INN). At each iteration, given the current set of explored points  $\mathcal{X}_e \in \mathcal{X}_0$ , an INN model is trained, which outputs the network uncertainty  $\mathcal{U}(x) = \bar{\Phi}(x) - \underline{\Phi}(x)$  over  $\mathcal{X}_0$ . Using Sherlock (Dutta et al., 2018a), a sample which maximizes the uncertainty,  $x^*$ , is obtained. Next, a local  $\delta$ -ball region,  $X^*$ , is sampled uniformly to be explored. The INN model is updated by including the newly explored samples. Finally, at the end of all iterations INN model (after  $M$  iterations) and  $\mathcal{X}_e$  are used to compute the lower bound of performance  $\Phi^l$ .

Performance guarantees in high dimensional spaces are computationally hard due to the inherent dependency on the sampling process. This necessitates an efficient uncertainty-guided sampling process, similar to Gaussian process regression but more scalable. To this end, we propose an efficient exploration strategy, followed by an exhaustive search that computes a lower performance bound. The above steps will rely on the neural-network verification tool SHERLOCK (Dutta et al., 2019a, 2018b). We use the following two-step process to estimate the lower bound outlined in the problem statement above.

1. **Active Learning Strategy:** This step learns an *Imprecise Neural Network (INN)*  $\{\underline{\Phi}(x), \bar{\Phi}(x)\}$ , which estimates the bounds on  $\psi(x_0)$  by drawing from samples  $x_0$  from  $\mathcal{X}_0$ . Explained in Section 4, INNs enable a novel notion of *network uncertainty* computed as the width  $w := [\bar{\Phi} - \underline{\Phi}](x)$ . We show that it satisfies the basic mathematical requirements of being an uncertainty measure. To implement efficient sampling in high dimensions, we propose an active learning strategy where SHERLOCK computes regions of high uncertainty in  $\mathcal{X}_0$  measured by the width  $w$ . Our active learning proceeds greedily by sampling points from high-uncertainty regions and using  $\psi$  to estimate the ground-truth performance. This sample-efficient active-learning process is termi-

nated after a finite number of steps. The explored regions help construct the set of distributions over which the guarantees in Eq. 1 hold.

2. **Computing Performance Limits:** The INN  $\{\underline{\Phi}(x), \overline{\Phi}(x)\}$  captures the upper and lower estimates of the performance function over a certain subset  $\mathcal{X}' \subseteq \mathcal{X}_0$  of the initial set  $\mathcal{X}_0$ . This subset  $\mathcal{X}'$  results from the exploration in the previous step. We aim to find a worst-case bound on the lower estimate of the INN over  $\mathcal{X}'$ , that is  $\Phi^l = \min_{x \in \mathcal{X}'} \underline{\Phi}(x)$ . We rely on SHERLOCK to compute  $\Phi^l$ , which serves as the lower bound over a set of distributions  $\mathcal{P}$ . We explain in Section 4.2 how to construct the set of probability distributions  $\mathcal{P}$  such that,  $\mathbb{E}_{X \sim P_{\mathcal{X}_0}} [P_{\psi(x_0)|X=x_0}(\psi(x_0) \geq \epsilon)] \geq (1 - \frac{1}{\lambda})$ ,  $\forall P_{\mathcal{X}_0} \in \mathcal{P}_{\mathcal{X}_0}$  and all conditional probabilities  $P_{\psi(x_0)|X=x_0}$  by setting  $\epsilon = \Phi^l$ .

### 3. Related Work

**Statistical guarantees for autonomy** Traditional approaches to statistical assurance are based on confidence intervals (Gupta et al., 2022; Alasmari et al., 2022) and hypothesis tests (Farid et al., 2022; Wang et al., 2021; Larsen and Legay, 2014). Recently though, due to its distribution-free nature, conformal prediction (CP) has become particularly popular (Luo et al., 2023; Cleaveland et al., 2022; Cairoli et al., 2021; Qin et al., 2021; Muthali et al., 2023; Qin et al., 2023). In short, it makes a statistical guarantee on the non-conformity score of the next sample given a calibration set (Vovk et al., 2005; Shafer and Vovk, 2008) — as long as the sample and the set are drawn exchangeably from some unknown distribution (without any assumptions on its shape or family). However, standard conformal prediction does not provide guarantees with respect to sets of distributions, so it has a limited ability to handle a distribution shift. Our experiments in Sec. 6 investigate the differences between the single-distribution CP setting and our robust formulation. Another recent work leverages random set theory to improve the sample efficiency and error bounds of sampling-based reachability (Lew et al., 2022), which would be interesting to combine with imprecise neural networks. An adjacent area is the testing and falsification of neural networks, which can be understood as an (often sampling-based) exploration of the network’s input-output relation (Du et al., 2022; Chakraborty and Bansal, 2023; Zhang et al., 2023; Dreossi et al., 2019), but aimed to satisfy the testing criteria (e.g., coverage) rather than establish performance guarantees.

**Uncertainty quantification and active learning** The goal of uncertainty quantification (Smith, 2013; Sullivan, 2015) is to compute a measure of trust towards a model’s output, with typical methods including Bayesian neural networks (Micheltore et al., 2020; Cardelli et al., 2019; Wicker et al., 2020), ensembles (Lakshminarayanan et al., 2017), confidence intervals (Park et al., 2021), and confidence calibration (Guo et al., 2017; Minderer et al., 2021). Gaussian processes (GPs) (Rasmussen and Williams, 2005) are a popular tool for data-driven modeling and uncertainty quantification in autonomy (Aoude et al., 2013; Bansal et al., 2018; Castaneda et al., 2021). They are commonly employed in state-of-the-art statistical verification methods to guide sampling based on Gaussian uncertainty (Qin et al., 2021; Moss et al., 2023; Petrov et al., 2022). Due to the challenges with scalability (Liu et al., 2020), GPs fall short as an uncertainty quantifier in high-dimensional black-box systems — shown in our experiments.

**Imprecision in Neural Networks** To effectively verify input-output properties on neural networks, set-based computation is typically implemented via overapproximation and abstractions (Dutta et al., 2018a; Sidrane et al., 2022; Gehr et al., 2018; Ashok et al., 2020; Ladner and Althoff, 2023). However, this setting is usually non-stochastic. To gauge uncertainty in the regression analysis at hand, techniques based on the imprecise probabilities literature (Troffaes and de Cooman, 2014;

Walley, 1991) have been developed. The most recent ones are Imprecise Bayesian Neural Networks (IBNNs) (Caprio et al., 2022), that give a principled way of carrying out a regression via credal sets, and Evidential Neural Networks (ENNs) (Denoeux, 2022), that instead use fuzzy logic.

## 4. Methodology

### 4.1. Preliminaries

In this section we detail the working of the proposed algorithm. To reiterate our goal, given an oracle function  $\psi : \mathcal{X} \rightarrow \mathbb{R}$ , we wish to compute a family of joint distributions  $\mathcal{P}$  and a lower bound  $\epsilon$  such that for any marginal distribution  $P_{\mathcal{X}_0}$  in  $\mathcal{P}_{\mathcal{X}_0}$ , the expectation that  $\psi(x_0) \geq \epsilon$ , for  $x_0 \sim P_{\mathcal{X}_0}$  is lower bounded by  $(1 - \frac{1}{\lambda})$ . Since,  $\psi$  is a black-box function, we use a regression based technique which estimates the function  $\psi$ . The model for our regression here is an Imprecise Neural Network (INN) which builds on standard DNNs. This is defined as the following,

**Definition 1 (Imprecise Neural Network)** *Given a set of deep neural networks  $\{f_1, f_2, \dots, f_k\}$  where  $f_i : \mathcal{X} \rightarrow \mathcal{Y}$ , an Imprecise Neural Network is given by a tuple  $\{\underline{\Phi}(x), \overline{\Phi}(x)\}$ , where  $\overline{\Phi}(x) = \max_{i \in [k]} f_i(x)$  and  $\underline{\Phi}(x) = \min_{i \in [k]} f_i(x)$ .*

In our case  $\mathcal{Y}$  is the set of reals  $\mathbb{R}$ . However, in a multi-dimensional case the *max/min* is taken element wise. The intention behind using INNs is that instead of computing the exact estimate of the ground-truth value, we wish to compute upper and lower bound estimates of the ground truth. This can be accomplished using a carefully crafted loss function shown in Equation 3. A salient feature that one derives from this is a novel way to quantify uncertainty, which is defined as follows:

**Definition 2 (Network Uncertainty)** *Given an Imprecise Neural Network  $\{\underline{\Phi}(x), \overline{\Phi}(x)\}$ , the uncertainty at  $x \in \mathcal{X}$  is defined as  $\mathcal{U}(x) = \overline{\Phi}(x) - \underline{\Phi}(x)$ .*

Hence, the larger the *disagreement* among the constituent networks that form the INN, the higher the uncertainty. This measure should be intuitive since, for parts of the space where no data was observed, randomly initialized DNNs are more likely to disagree. We further justify the choice of using this width as a measure of uncertainty in Section 5.1.

**Optimization over DNN** Next, we consider the problem of optimizing the inputs to a deep neural network with an objective to maximize/minimize the output. Exact solutions of this problem are generally hard due to its NP-complete nature (Katz et al., 2017). However, due to the considerable utility of solving this problem in the context of verifying of neural networks, this has received much attention (Elboher et al., 2019; Fazlyab et al., 2019; Dutta et al., 2019b; Tran et al., 2020; Ivanov et al., 2021). In this paper, we use one such neural network verification tool SHERLOCK (Dutta et al., 2019a) which uses a mixed integer linear program (MILP) encoding of a DNN, with gradient guided search to solve this optimization problem. At a high-level for  $x \in$  convex set  $S$ , and  $f_i$  a DNN, SHERLOCK can compute an interval  $[m, M]$ , where  $m = \min_{x \in S} f_i(x)$  and  $M = \max_{x \in S} f_i(x)$ .

Extension of this search to an INN is straightforward. This is because the output of an INN simply chooses the maxima/minima over a finite number  $[k]$  of constituent DNNs.

### 4.2. Algorithms

In general, estimating the nature of  $\psi$  by sampling densely over a space of higher dimensions ( $> 10$ ) is computationally intractable. This means that virtually any algorithm would gain from an effi-

cient sampling schema. In the literature, sample efficiency often involves *forward*-looking techniques, like those using Gaussian processes that sample first and then assess uncertainty estimates. However, our approach adopts a *backward* looking technique, allowing the learner to generate query points  $x_0 \in \mathcal{X}_0$  based on its intrinsic curiosity. This paradigm is similar to Active Learning (AL) (Burbidge et al., 2007) in the literature.

In AL, the learner accesses an oracle function to query for ground truth labels instead of relying on a labeled training dataset. Due to the costly nature of these queries, the learner aims to minimize their number. In the standard active-learning setting, a common assumption is that the learner has access to a finite set of unlabeled input samples. However, in our setting, this assumption does not hold. As stated before, the learner proposes new points to sample from a real-valued compact set  $\mathcal{X}_0$ , where the input samples are drawn from. This is captured in the *active learning algorithm* (Algorithm 1). The learner samples different regions of the input space, depending on the uncertainty expressed by the INN.

**Algorithm for Active Learning** As shown in Algorithm 1, the INN  $\{\underline{\Phi}(x), \overline{\Phi}(x)\}$  is randomly initialized with some starting distribution and trained using the loss function outlined in Equation 3. Next, at each iteration (Lines 4 – 9), we use SHERLOCK to obtain a point  $x^*$  which maximizes the uncertainty  $\mathcal{U}(x) = \overline{\Phi}(x) - \underline{\Phi}(x)$  in the INN’s predictions. We sample uniformly from a  $\delta$ -ball ( $\mathcal{X}^*$ ) centered at  $x^*$ , and obtain its labels using an oracle function  $\psi$ . Next, (Lines 7 – 8) we incorporate these samples into our current training set and retrain the INN. At the end of active-learning, the explored region  $\mathcal{X}_e$  is returned as a union of intervals in the space  $\mathcal{X}$ . We maintain this representation of  $\mathcal{X}_e$  for ease of implementation of the subsequent algorithms.

**Algorithm for Computing Performance Limits**

The aim of Algorithm 2 is to find the lowest estimate  $\underline{\Phi}(x)$  assigned by the INN. This again is an NP-complete problem and can be computationally challenging. However, we can use SHERLOCK to compute this minima for different regions explored in the sampling process when building the set  $\mathcal{X}_e$ . This is captured in Line 3, where the local minima is computed by solving  $\min_{x \in \mathcal{X}'} \underline{\Phi}(x)$ , for a subset  $\mathcal{X}'$  in  $\mathcal{X}_e$ . We perform this repeatedly in the loop (Lines 2 – 5), and compute the *INN-minima* over all such values (Line 6). We return this INN-minima after

---

**Algorithm 1** Active Learning

---

**Input:** Oracle function  $\psi$ , set  $\mathcal{X}_0$ ,  
**Output:** An INN  $\{\underline{\Phi}(x), \overline{\Phi}(x)\}$ , explored set  $\mathcal{X}_e$   
**Parameters:** **Iteration Count** :  $M$ ,  
**Neighborhood Size** :  $\delta$

- 1:  $\mathcal{T} := \{(x_i, y_i)\}_{i=1}^N \leftarrow$  Draw samples from  $\mathcal{X}_0$ , and assign labels using  $\psi$   
 {These samples can be picked according to some desirable starting distribution as well. }
- 2:  $\{\underline{\Phi}(x), \overline{\Phi}(x)\} \leftarrow$  Train INN on  $\mathcal{T}$  using Eqn. 3
- 3:  $\mathcal{X}_e = \mathcal{X}_0$
- 4: **for**  $k = 1$  to  $M$  **do**
- 5:    $x^* \leftarrow$  Maximize Uncertainty  $\mathcal{U}$  in INN
- 6:    $\mathcal{T}^* := \{(x_i, y_i)\}_{i=1}^N \leftarrow$  Draw samples uniformly from set  $\mathcal{X}^* = \{x : \|x - x^*\|_\infty \leq \delta\}$ , and assign labels using  $\psi$
- 7:    $\mathcal{X}_e = \mathcal{X}_e \cup \mathcal{X}^*$  and  $\mathcal{T} = \mathcal{T} \cup \mathcal{T}^*$
- 8:    $\{\underline{\Phi}(x), \overline{\Phi}(x)\} \leftarrow$  Retrain INN on  $\mathcal{T}$  using loss in Equation 3
- 9: **end for**
- 10: **return**  $\{\underline{\Phi}(x), \overline{\Phi}(x)\}, \mathcal{X}_e$

---



---

**Algorithm 2** Compute Performance Limits

---

**Input:** INN  $\{\underline{\Phi}(x), \overline{\Phi}(x)\}$ , explored set  $\mathcal{X}_e$   
**Output:** Lower bound  $\Phi^l$

- 1:  $C = \phi$
- 2: **for** subset  $\mathcal{X}' \subseteq \mathcal{X}_e$  **do**
- 3:   local-minima  $\leftarrow$  Compute minima of INN  $\{\underline{\Phi}(x), \overline{\Phi}(x)\}$  in set  $\mathcal{X}'$
- 4:    $C = C \cup$  local-minima
- 5: **end for**
- 6: INN-Minima = Compute lowest value in  $C$
- 7: **return** INN-Minima -  $\lambda\beta$

---

subtracting the  $\lambda\beta$  term, as outlined in Theorem 3.

**Constructing the family of distributions** We define the family of distributions over  $\mathcal{X}$  in our analysis as follows. Note that due to the nature of Algorithm 1, the explored set can be expressed as a union over finite number of subsets,  $\mathcal{X}_e = \mathcal{X}_1 \cup \dots \cup \mathcal{X}_m$ . Let  $u_j$  denote the pdf of the uniform distribution over  $\mathcal{X}_j$ , for all  $j \in \{1, \dots, m\}$ . Then, consider probability measure  $\tilde{P}$  whose pdf  $\tilde{p}$  is given by a (convex) mixture of the uniforms. That is,  $\tilde{p}(x) = \sum_{j=1}^m \gamma_j u_j(x)$ , for all  $x \in \mathcal{X}$ , and a collection of coefficients  $\{\gamma_j\}$  whose elements are nonnegative and sum up to 1. Our family is defined as  $\mathcal{P}_{\mathcal{X}} := \{P_X : P_X = (1 - \alpha)\tilde{P} + \alpha Q, \text{ where } Q \text{ is any distribution on } \mathcal{X}\}$ , for some  $\alpha \in (0, 1)$ . This is called a  $\alpha$ -contaminated class (Caprio et al., 2023; Huber and Ronchetti, 2009). Notice that, as a result, the uniform over the whole  $\mathcal{X}$  is included in  $\mathcal{P}_{\mathcal{X}}$ . We have that the upper probability  $\bar{P}_X$  – formally introduced in the next section – is given by  $\bar{P}_X = (1 - \alpha)\tilde{P} + \alpha$  (Wasserman and Kadane, 1990, Example 3).

## 5. Theory

Recall that a *credal set* is a convex set of probabilities. It is called a *finitely generated credal set* if it has finitely many extreme elements.<sup>1</sup> For a given set  $\mathcal{P}$  of probabilities on a generic measurable space  $(\Omega, \mathcal{F})$ , its *upper probability* is defined as the upper envelope, that is,  $\bar{P}(A) := \sup_{P \in \mathcal{P}} P(A)$ , for all  $A \in \mathcal{F}$ . Similarly, the *lower probability* is the lower envelope, that is,  $\underline{P}(A) := \inf_{P \in \mathcal{P}} P(A)$ , for all  $A \in \mathcal{F}$ . In addition, upper and lower probabilities are conjugate to each other, i.e.  $\bar{P}(A) = 1 - \underline{P}(A^c)$ , for all  $A \in \mathcal{F}$ .

Call  $(\mathcal{X}, \mathcal{A}_{\mathcal{X}})$  the measurable space of inputs and  $(\mathcal{Y}, \mathcal{A}_{\mathcal{Y}})$  the measurable space of outputs. Consider a set of probability measures  $\mathcal{P}$  on  $(\mathcal{X} \times \mathcal{Y}, \mathcal{A}_{\mathcal{X} \times \mathcal{Y}})$ . Suppose that every element  $P$  in  $\mathcal{P}$  can be decomposed as  $P(X, Y) = P(X)P(Y | X) \equiv P_X(X)P_{Y|X}(Y)$ . This entails that  $\mathcal{P}$  can be decomposed in  $\mathcal{P}_{\mathcal{X}}$  and  $\mathcal{P}_{\mathcal{Y}|\mathcal{X}}$ , that is, for every  $P \in \mathcal{P}$ , we can find  $P_X \in \mathcal{P}_{\mathcal{X}}$  and  $P_{Y|X} \in \mathcal{P}_{\mathcal{Y}|\mathcal{X}}$  such that  $P(X, Y) = P_X(X)P_{Y|X}(Y)$ . In turn, this implies that we can write the lower probability  $\underline{P}$  associated with  $\mathcal{P}$  as the product of the lower probability  $\underline{P}_X$  associated with  $\mathcal{P}_{\mathcal{X}}$  and the lower probability  $\underline{P}_{Y|X}$  associated with  $\mathcal{P}_{\mathcal{Y}|\mathcal{X}}$ . Similarly, this is true for upper probability  $\bar{P}$ . Notice that we implicitly consider geometric conditioning (Gong and Meng, 2021), that is,

$$\underline{P}_{Y|X}(Y) = \frac{\underline{P}(X, Y)}{\underline{P}_X(X)}, \quad (2)$$

and similarly for upper probabilities. We assume that the true joint distribution is in  $\mathcal{P}$ , the true marginal for  $X$  is in  $\mathcal{P}_{\mathcal{X}}$  and the true conditional is in  $\mathcal{P}_{\mathcal{Y}|\mathcal{X}}$ .

Consider the following loss function, an imprecise version of (Oala et al., 2020, Equation (2)),

$$\begin{aligned} \mathcal{L}(\underline{\Phi}, \bar{\Phi}) := & \sup_{P_X \in \mathcal{P}_{\mathcal{X}}} \int_{\mathcal{X}} \left[ \sup_{P_{Y|X} \in \mathcal{P}_{\mathcal{Y}|\mathcal{X}}} \int_{\mathcal{Y}} \max(y - \bar{\Phi}(x), 0)^2 P_{Y|X}(dy) \right. \\ & \left. + \sup_{P_{Y|X} \in \mathcal{P}_{\mathcal{Y}|\mathcal{X}}} \int_{\mathcal{Y}} \max(\underline{\Phi}(x) - y, 0)^2 P_{Y|X}(dy) + \beta (\bar{\Phi}(x) - \underline{\Phi}(x)) \right] P_X(dx), \end{aligned} \quad (3)$$

where  $\beta > 0$  is the tightness parameter. Using a loss function that comprises credal sets allows to account for the worst case scenario, and so to obtain a more conservative but more robust outcome. To ease notation, (3) can be rewritten as

$$\mathcal{L}(\underline{\Phi}, \bar{\Phi}) := \bar{\mathbb{E}}_X \left[ \bar{\mathbb{E}}_{Y|X}(\bar{m}^2) + \bar{\mathbb{E}}_{Y|X}(\underline{m}^2) + \beta (\bar{\Phi}(x) - \underline{\Phi}(x)) \right], \text{ where,}$$

1. The extreme elements are the ones that cannot be written as a convex combination of one another.

- $\bar{m} := \max(y - \bar{\Phi}(x), 0)$ ,  $\underline{m} := \max(\Phi(x) - y, 0)$ ,  $\mathbb{E}_{Y|X}(\bar{m}^2) := \int_{\mathcal{Y}} \max(y - \bar{\Phi}(x), 0)^2 P_{Y|X}(\mathrm{d}y)$ ,  
 $\mathbb{E}_{Y|X}(\underline{m}^2) := \int_{\mathcal{Y}} \max(\Phi(x) - y, 0)^2 P_{Y|X}(\mathrm{d}y)$ ,
- for a generic functional  $g$  on  $\mathcal{Y}$ ,  $\bar{\mathbb{E}}_{Y|X}(g) := \sup_{P_{Y|X} \in \mathcal{P}_{\mathcal{Y}|X}} \int_{\mathcal{Y}} g(y) P_{Y|X}(\mathrm{d}y)$ ,
- for a generic functional  $f$  on  $\mathcal{X}$ ,  $\bar{\mathbb{E}}_X(f) := \sup_{P_X \in \mathcal{P}_X} \int_{\mathcal{X}} f(x) P_X(\mathrm{d}x)$ .

**Theorem 3** *Pick any  $\lambda > 0$  and any pair  $(x, y)$  sampled from a distribution in  $\mathcal{P}$ . Let  $A = \{\Phi(x) - \lambda\beta \leq y \leq \bar{\Phi}(x) + \lambda\beta\}$ . If  $\mathcal{P}_X$  and  $\mathcal{P}_{Y|X}$  are compact, then<sup>2</sup>*

$$\mathbb{E}_X \left[ \underline{P}_{Y|X}(A) \right] = \inf_{P_X \in \mathcal{P}_X} \int_{\mathcal{X}} \underline{P}_{Y|X}(\{\Phi(x) - \lambda\beta \leq y \leq \bar{\Phi}(x) + \lambda\beta\}) P_X(\mathrm{d}x) \geq 1 - \frac{1}{\lambda}.$$

The Proof is in the Appendix A.1, of Dutta et al. (2023). We have two corollaries.

**Corollary 4** *Pick any  $\lambda > 0$  and any pair  $(x, y)$  sampled from a distribution in  $\mathcal{P}$ . Let  $A = \{\Phi(x) - \lambda\beta \leq y \leq \bar{\Phi}(x) + \lambda\beta\}$ . If  $\mathcal{P}_X$  and  $\mathcal{P}_{Y|X}$  are compact, then  $\bar{\mathbb{E}}_X[\underline{P}_{Y|X}(A)] - \mathbb{E}_X[\underline{P}_{Y|X}(A)] \leq \frac{1}{\lambda}$ .*

**Corollary 5** *Pick any  $\lambda, \alpha > 0$  and any pair  $(x, y)$  sampled from a distribution in  $\mathcal{P}$ . If  $\mathcal{P}_X$  and  $\mathcal{P}_{Y|X}$  are compact, then  $\bar{\mathbb{E}}_X[\mathbf{1}\{\bar{P}_{Y|X}(y < \Phi(x) - \lambda\beta, y > \bar{\Phi}(x) + \lambda\beta) > \alpha\}] \leq \frac{1}{\lambda\alpha}$ , where  $\mathbf{1}\{\cdot\}$  denotes the indicator function.*

From an applied point of view, the requirements of  $\mathcal{P}_X$  and  $\mathcal{P}_{Y|X}$  being compact are easy to satisfy. For instance, it is enough for them to be finite sets or finitely generated credal sets.

## 5.1. INN Uncertainty

In this work, we are interested in the input elements  $x \in \mathcal{X}$  whose *network uncertainty* is high. The latter is defined as  $\mathcal{U}(x) = \bar{\Phi}(x) - \Phi(x)$ . After training, we use SHERLOCK to sample elements from regions of the input space  $\mathcal{X}$  where the network uncertainty is maximal. By doing this, our aim is that of exploring the regions of  $\mathcal{X}$  that we do not observe during training. We call this endeavor *input space curiosity*. Let us note in passing that network uncertainty is a good measure of uncertainty both from an intuitive and a mathematical viewpoint. Intuitively, we have the highest  $\mathcal{U}(x)$  for the elements  $x \in \mathcal{X}$  that the neural networks disagree about the most. This conveys the idea of (high) uncertainty. Mathematically, we have that

- (1)  $0 \leq \mathcal{U}(x) < \infty$ , for all  $x \in \mathcal{X}$ ;
- (2)  $\mathcal{U}(x)$  corresponds to the Lebesgue measure of the segment  $[\Phi(x), \bar{\Phi}(x)]$ , and is therefore a continuous functional.
- (3)  $\mathcal{U}(x)$  is monotone. To see this, let  $x, x' \in \mathcal{X}$  and suppose that  $\Phi(x') \leq \Phi(x)$  and  $\bar{\Phi}(x') \geq \bar{\Phi}(x)$ . Then,  $[\Phi(x), \bar{\Phi}(x)] \subseteq [\Phi(x'), \bar{\Phi}(x')]$  and  $\mathcal{U}(x) \leq \mathcal{U}(x')$ .
- (4)  $\mathcal{U}(x)$  exhibits probability consistency. That is, if  $\Phi(x) = \bar{\Phi}(x)$ , then  $\mathcal{U}(x) = 0$ .

As pointed out by Abellán and Klir (2005) and Jiroušek and Shenoy (2018), a suitable measure of credal uncertainty should satisfy properties (1)-(4). Although interval  $[\Phi(x), \bar{\Phi}(x)]$  is not a credal set, it is heuristically similar to an interval of measure (IoM). In the theory of IoM's, it is assumed that the true pdf/pmf  $p^*$  of interest is such that  $p^*(x) \in [\ell(x), u(x)]$ , for all  $x$ , where  $\ell$  and  $u$  are the lower and upper pdf/pmf's, respectively. In turn, Coolen (1992) and Wasserman (1992) remark how

2. Here and in the rest of the paper, compact has to be understood with respect to the topologies  $\sigma(\text{ba}(\mathcal{A}_X); B(\mathcal{A}_X))$  and  $\sigma(\text{ba}(\mathcal{A}_Y); B(\mathcal{A}_Y))$ , respectively. Recall that  $\text{ba}(\Sigma)$  is the set of all bounded finitely additive (signed) measures on a generic sigma-algebra  $\Sigma$ , and  $B(\Sigma)$  is the set of all bounded and  $\Sigma$ -measurable functions.



an IoM can be thought of as a neighborhood of a probability measure, which is itself a credal set. This heuristic connection between  $[\underline{\Phi}(x), \overline{\Phi}(x)]$  and credal sets explains why  $\mathcal{U}(\cdot)$  satisfying (1)-(4) is an indicator of it being a good uncertainty measure.

## 6. Experimental Evaluation

In this section, we experimentally evaluate our INN-based probabilistic guarantees for closed-loop interactions between a black-box simulator and a reinforcement learning-based control policy. We aim to establish a lower bound on the expected performance score and construct a set of distributions where the guarantee holds. Our approach handles systems of dimensionality greater than 10 and ensures coverage guarantees.

**Environments** We consider the complete set of 10 environments from the Mujoco tasks in the OpenAI control suite (Brockman et al., 2016). The control policy is trained using DDPG algorithm (for details, Appendix B, Dutta et al. (2023)). We initialize and simulate the environments until termination and compute the temporal average of the reward as  $R_{avg} = \frac{1}{T} \sum_{i=1}^T r_i$ . Here,  $r_i$  is the reward at time step  $i$ , and  $T$  is the duration of the episode. In our experiments we set the confidence parameter to 95% by choosing  $\lambda = 20$ . For the INN, we select  $k = 3$  DNNs. Each DNN is a 2 layer feedforward neural network with a width of 50 and ReLU activation. The width of the exploration set  $\delta$  is set to 0.05, which is half of the full range picked by the Mujoco suite developers. The number of iterations of active learning is set to  $M = 20$ . We draw  $N = 200$  samples each time we sample a local region (Algorithm 1, Line 6). The execution time of the proposed algorithms is presented in Table 8 of the Appendix in Dutta et al. (2023). With varying dimensionality of the benchmark and interval size.

**Computing Performance Lower Bounds** We wish to compute the lower bound  $\epsilon$  on the performance function  $R_{avg}$ . The bounds  $(\underline{\Phi}(x) - \lambda\beta)$  computed using Algorithm 2 are presented in Table 1.  $4.2k$  samples are used to train the INN. The validity of the lower bounds predicted by the INN is checked empirically against  $20k$  samples uniformly from the initial set  $\mathcal{X}_0$ . We compute the fraction of times the simulations return a value above the INN proposed lower limit from this sample set. This fraction is presented in Table 1, as percentage coverage, and repeated for different  $\beta$ . We observe that for all the environments, more than 99% of the samples return  $R_{avg}$  values above the predicted score.

**Comparison with Conformal Prediction** We compare our method to inductive conformal prediction (ICP), a variant of CP designed to improve computational efficiency (Papadopoulos et al., 2002; Vovk et al., 2005). Given a model  $f$  trained on set  $\mathcal{X}_{tr} \sim P_{\mathcal{X}}$ , a calibration set  $\mathcal{X}_{cal} \sim P_{\mathcal{X}}$ , a non-conformity score function  $s$ , for confidence level  $\alpha \in (0, 1)$ , ICP produces a prediction region  $C(x_{te})$  such that  $P(y_{te} \in C(x_{te})) \geq 1 - \alpha$ . The non-conformity score captures the quality of a model’s prediction (e.g.,  $s(x, y) = |y - f(x)|$  for an input  $x$  and its ground-truth target  $y$ ). In our experiments, the final set of explored states  $\mathcal{X}_e$  is divided into a training and calibration set for CP ( $\mathcal{X}_e = \mathcal{X}_{tr} \cup \mathcal{X}_{cal}$ ). The CP prediction intervals capture the uncertainty in the estimates of the perfor-

Environment	$\mathcal{X}$ Dim	$\beta = 10^{-4}$		$\beta = 10^{-3}$		$\beta = 10^{-2}$	
		Lower Bound	Cov. (%)	Lower Bound	Cov. (%)	Lower Bound	Cov. (%)
Ant	29	-1.29	99.9	-1.58	100	-0.98	99.3
Half-Cheetah	18	3.97	100	9.1	99.8	8.71	99.8
Hopper	12	1.4	99.9	1.45	99.8	1.46	99.8
Humanoid	47	4.72	100	4.5	100	4.99	99.1
Humanoid-Standup	47	121.2	99.7	100	100	143.6	99.4
Inverted Double Pend.	6	6.4	100	9.1	100	8.94	100
Inverted Pendulum	4	0.64	100	0.98	100	0.8	100
Reacher	8	-0.08	100	-0.1	100	-0.28	100
Swimmer	10	0.13	100	0.12	100	-0.06	100
Walker2d	18	0.62	99.5	0.35	99.7	0.25	99.7

Table 1: We estimate the lower limit on  $R_{avg}$  using the proposed INN method, and compare it with  $20k$  samples drawn uniformly from the whole initial set  $\mathcal{X}_0$ . We observe that the fraction of samples which satisfy the estimated lower bounds (i.e., coverage ‘‘Cov.’’) are well above the 95% target. Here,  $\mathcal{X}$  denotes the input space.

mance  $R_{avg}$ . Generally, CP algorithms can be restrictive as they typically require that the test data be drawn from the same distribution as the training data (i.e.,  $x_{te} \sim P_{\mathcal{X}}$ ). This can be difficult to guarantee in practice. Therefore in our experiments, we compare the quality of the prediction intervals produced by our INN model to those of ICP in terms of prediction coverage and size. We evaluate the methods under two settings: (1) **In-distribution Evaluation**: Test samples are drawn from a uniform distribution matching the training distribution for INNs and ICP. The 95% confidence regions proposed by ICP are compared to the INN intervals computed as  $[\underline{\Phi}(x) - \lambda\beta, \overline{\Phi}(x) + \lambda\beta]$ . (2) **Out-of-distribution Evaluation**: Test samples are drawn from a uniform distribution NOT matching the training distribution. Note, that the training distribution is a mixture of uniform distributions over specific intervals in the input space. The testing samples are sampled uniformly over the entire input space.

The results of in-distribution evaluation are presented in Table 2. We observe that the prediction regions proposed by the INN have a higher coverage rate, while the coverage guarantees for CP do not hold precisely in some cases. However, this comes at the cost of larger width of the INN intervals for some cases. For the out-of-distribution evaluation, in order for the guarantees of CP to hold, the test distribution cannot be drawn uniformly from the entire input space  $\mathcal{X}_0$ . In comparison, as discussed in Section 4, the uniform distribution over the entire set is covered in our family of distributions. The ramifications of this can be observed in Table 3. The prediction regions of CP violate the coverage guarantees while intervals proposed with our INN method has a coverage rate above 95%.

Environment	$\mathcal{X}$ Dim	CP		INN (ours)	
		Cov. (%)	Interval Size	Cov. (%)	Interval Size
Ant	29	93	3.2	99	4.2
Half-Cheetah	18	93	$4.9 \times 10^{-1}$	100	3
Hopper	12	97	2.9	100	2.2
Humanoid	47	97	2.7	100	3
Humanoid-Standup	47	96	143	99	260
Inverted Double Pend.	6	95	$6.7 \times 10^{-3}$	100	$5.1 \times 10^{-2}$
Inverted Pendulum	4	95	$1.2 \times 10^{-3}$	100	$4.1 \times 10^{-2}$
Reacher	8	93	$3.3 \times 10^{-2}$	100	$7.6 \times 10^{-2}$
Swimmer	10	93	$2.8 \times 10^{-3}$	100	$4.9 \times 10^{-2}$
Walker2d	18	95	5.2	99	5.8

Table 2: We compare the coverage rates (“Cov.”) and size of prediction regions between an INN and CP for  $\beta = 10^{-3}$  when the test samples are in-distribution.  $\mathcal{X}$  denotes the input space. The interval size of the INN is an average value across the samples.

Environment	$\mathcal{X}$ Dim	CP		INN (ours)	
		Cov. (%)	Interval Size	Cov. (%)	Interval Size
Ant	29	94	3.2	100	4.3
Half-Cheetah	18	93	$4.9 \times 10^{-1}$	100	1.9
Hopper	12	97	2.9	100	2.5
Humanoid	47	98	2.7	99	2.8
Humanoid-Standup	47	95	143	100	262
Inverted Double Pend.	6	94	$6.7 \times 10^{-3}$	100	$5.1 \times 10^{-2}$
Inverted Pendulum	4	100	$1.2 \times 10^{-3}$	100	$4.2 \times 10^{-2}$
Reacher	8	91	$3.3 \times 10^{-2}$	100	$8.5 \times 10^{-2}$
Swimmer	10	92	$2.8 \times 10^{-3}$	100	$5 \times 10^{-2}$
Walker2d	18	94	5.2	99	5.2

Table 3: We compare the coverage rates (“Cov.”) and size of prediction regions between an INN and CP for  $\beta = 10^{-3}$  when the test samples are out-of-distribution.  $\mathcal{X}$  denotes the input space. The interval size of the INN is an average value across the samples.

**Ablations** We perform further ablations on different values of  $\beta \{10^{-2}, 10^{-4}\}$ , presented in Table 4, and Table 5 in Appendix B of Dutta et al. (2023). We observe similar trends wherein the INN has better coverage guarantees but is more conservative.

## 6.1. Conclusion

In this paper, we show that statistical guarantees can step outside of the limitations of being restricted to a single distribution. We validate this claim experimentally by demonstrating this over state-of-the-art high-dimensional case studies commonly explored in the reinforcement learning literature. The bounds estimated hold in both the in-distribution and out-of-distribution cases. In the future, we plan to explore more efficient ways to perform active learning that can avoid expensive queries to a neural-network verification tool.

## References

- Joaquín Abellán and George J. Klir. Additivity of uncertainty measures on credal sets. *International Journal of General Systems*, 34(6):691–713, 2005.
- Naif Alasmari, Radu Calinescu, Colin Paterson, and Raffaella Mirandola. Quantitative verification with adaptive uncertainty reduction. *Journal of Systems and Software*, 188:111275, June 2022. ISSN 0164-1212. doi: 10.1016/j.jss.2022.111275. URL <https://www.sciencedirect.com/science/article/pii/S016412122200036X>.
- Georges S. Auode, Brandon D. Luders, Joshua M. Joseph, Nicholas Roy, and Jonathan P. How. Probabilistically safe motion planning to avoid dynamic obstacles with uncertain motion patterns. *Autonomous Robots*, 35(1):51–76, July 2013. ISSN 1573-7527. doi: 10.1007/s10514-013-9334-3. URL <https://doi.org/10.1007/s10514-013-9334-3>.
- Pranav Ashok, Vahid Hashemi, Jan Křetínský, and Stefanie Mohr. DeepAbstract: Neural Network Abstraction for Accelerating Verification. In Dang Van Hung and Oleg Sokolsky, editors, *Automated Technology for Verification and Analysis*, Lecture Notes in Computer Science, pages 92–107, Cham, 2020. Springer International Publishing. ISBN 978-3-030-59152-6. doi: 10.1007/978-3-030-59152-6\_5.
- Somil Bansal, Shromona Ghosh, Alberto Sangiovanni-Vincentelli, Sanjit A. Seshia, and Claire J. Tomlin. Context-Specific Validation of Data-Driven Models. *arXiv:1802.04929 [cs]*, February 2018. URL <http://arxiv.org/abs/1802.04929>. arXiv: 1802.04929.
- Greg Brockman, Vicki Cheung, Ludwig Pettersson, Jonas Schneider, John Schulman, Jie Tang, and Wojciech Zaremba. OpenAI Gym, June 2016. URL <http://arxiv.org/abs/1606.01540>. arXiv:1606.01540 [cs].
- Robert Burbidge, Jem J. Rowland, and Ross D. King. Active learning for regression based on query by committee. In Hujun Yin, Peter Tino, Emilio Corchado, Will Byrne, and Xin Yao, editors, *Intelligent Data Engineering and Automated Learning - IDEAL 2007*, pages 209–218, Berlin, Heidelberg, 2007. Springer Berlin Heidelberg. ISBN 978-3-540-77226-2.
- Francesca Cairolì, Luca Bortolussi, and Nicola Paoletti. Neural predictive monitoring under partial observability. In Lu Feng and Dana Fisman, editors, *Runtime Verification*, pages 121–141, Cham, 2021. Springer International Publishing. ISBN 978-3-030-88494-9.
- Michele Caprio, Souradeep Dutta, Radoslav Ivanov, Kuk Jang, Vivian Lin, Oleg Sokolsky, and Insup Lee. Imprecise Bayesian neural networks. *Submitted to AAAI 2023*, 2022.
- Michele Caprio, Yusuf Sale, Eyke Hüllermeier, and Insup Lee. A novel Bayes’ theorem for upper probabilities. *Available at arXiv:2307.06831*, 2023.
- Luca Cardelli, Marta Kwiatkowska, Luca Laurenti, Nicola Paoletti, Andrea Patane, and Matthew Wicker. Statistical Guarantees for the Robustness of Bayesian Neural Networks. pages 5693–5700, 2019. URL <https://www.ijcai.org/proceedings/2019/789>.

- Fernando Castaneda, Jason J. Choi, Bike Zhang, Claire J. Tomlin, and Koushil Sreenath. Pointwise Feasibility of Gaussian Process-based Safety-Critical Control under Model Uncertainty. In *2021 60th IEEE Conference on Decision and Control (CDC)*, pages 6762–6769, December 2021. doi: 10.1109/CDC45484.2021.9683743. ISSN: 2576-2370.
- Kaustav Chakraborty and Somil Bansal. Discovering Closed-Loop Failures of Vision-Based Controllers via Reachability Analysis. *IEEE Robotics and Automation Letters*, 8(5):2692–2699, May 2023. ISSN 2377-3766. doi: 10.1109/LRA.2023.3258719. Conference Name: IEEE Robotics and Automation Letters.
- Matthew Cleaveland, Lars Lindemann, Radoslav Ivanov, and George J. Pappas. Risk verification of stochastic systems with neural network controllers. *Artificial Intelligence*, 313:103782, 2022. ISSN 0004-3702. doi: <https://doi.org/10.1016/j.artint.2022.103782>. URL <https://www.sciencedirect.com/science/article/pii/S0004370222001229>.
- Frank P. A. Coolen. Imprecise highest density regions related to intervals of measures. *Memorandum COSOR*, 9254, 1992.
- Anthony Corso, Robert Moss, Mark Koren, Ritchie Lee, and Mykel Kochenderfer. A Survey of Algorithms for Black-Box Safety Validation of Cyber-Physical Systems. *Journal of Artificial Intelligence Research*, 72:377–428, January 2022. ISSN 1076-9757. doi: 10.1613/jair.1.12716. URL <https://dl.acm.org/doi/10.1613/jair.1.12716>.
- Thierry Denoeux. An evidential neural network model for regression based on random fuzzy numbers. Available at [arXiv:2208.00647](https://arxiv.org/abs/2208.00647), 2022.
- Mohammad Divband Soorati, Enrico H. Gerding, Enrico Marchioni, Pavel Naumov, Timothy J. Norman, Sarvapali D. Ramchurn, Bahar Rastegari, Adam Sobey, Sebastian Stein, Danesh Tarpore, Vahid Yazdanpanah, Jie Zhang, Stefano V. Albrecht, and Michael Woolridge. From intelligent agents to trustworthy human-centred multiagent systems. *AI Communications*, 35(4):443–457, January 2022. ISSN 0921-7126. doi: 10.3233/AIC-220127. URL <https://doi.org/10.3233/AIC-220127>.
- Tommaso Dreossi, Daniel J. Fremont, Shromona Ghosh, Edward Kim, Hadi Ravanbakhsh, Marcell Vazquez-Chanlatte, and Sanjit A. Seshia. VERIFAI: A Toolkit for the Design and Analysis of Artificial Intelligence-Based Systems. *arXiv:1902.04245 [cs]*, February 2019. URL <http://arxiv.org/abs/1902.04245>. arXiv: 1902.04245.
- Xuefeng Du, Zhaoning Wang, Mu Cai, and Yixuan Li. VOS: Learning What You Don’t Know by Virtual Outlier Synthesis. 2022. URL <https://openreview.net/forum?id=TW7d65uYu5M>.
- Souradeep Dutta, Susmit Jha, Sriram Sankaranarayanan, and Ashish Tiwari. Output Range Analysis for Deep Feedforward Neural Networks. In Aaron Dutle, César Muñoz, and Anthony Narkawicz, editors, *NASA Formal Methods*, Lecture Notes in Computer Science, pages 121–138, Cham, 2018a. Springer International Publishing. ISBN 978-3-319-77935-5. doi: 10.1007/978-3-319-77935-5\_9.

- Souradeep Dutta, Susmit Jha, Sriram Sankaranarayanan, and Ashish Tiwari. Output range analysis for deep feedforward neural networks. In Aaron Dutle, César Muñoz, and Anthony Narkawicz, editors, *NASA Formal Methods*, pages 121–138, Cham, 2018b. Springer International Publishing. ISBN 978-3-319-77935-5.
- Souradeep Dutta, Xin Chen, Susmit Jha, Sriram Sankaranarayanan, and Ashish Tiwari. Sherlock - a tool for verification of neural network feedback systems: Demo abstract. HSCC '19, page 262–263, New York, NY, USA, 2019a. Association for Computing Machinery. ISBN 9781450362825. doi: 10.1145/3302504.3313351. URL <https://doi.org/10.1145/3302504.3313351>.
- Souradeep Dutta, Xin Chen, and Sriram Sankaranarayanan. Reachability analysis for neural feedback systems using regressive polynomial rule inference. In *Proceedings of the 22nd ACM International Conference on Hybrid Systems: Computation and Control*, HSCC '19, pages 157–168, New York, NY, USA, April 2019b. Association for Computing Machinery. ISBN 978-1-4503-6282-5. doi: 10.1145/3302504.3311807. URL <https://doi.org/10.1145/3302504.3311807>.
- Souradeep Dutta, Michele Caprio, Vivian Lin, Matthew Cleaveland, Kuk Jin Jang, Ivan Ruchkin, Oleg Sokolsky, and Insup Lee. Distributionally robust statistical verification with imprecise neural networks, 2023. URL <https://arxiv.org/abs/2308.14815>.
- Yizhak Yisrael Elboher, Justin Gottschlich, and Guy Katz. An Abstraction-Based Framework for Neural Network Verification. October 2019. URL <http://arxiv.org/abs/1910.14574>. arXiv: 1910.14574.
- Alec Farid, Sushant Veer, and Anirudha Majumdar. Task-Driven Out-of-Distribution Detection with Statistical Guarantees for Robot Learning. In *Proceedings of the 5th Conference on Robot Learning*, pages 970–980. PMLR, January 2022. URL <https://proceedings.mlr.press/v164/farid22a.html>. ISSN: 2640-3498.
- Mahyar Fazlyab, Manfred Morari, and George J. Pappas. Probabilistic Verification and Reachability Analysis of Neural Networks via Semidefinite Programming. In *2019 IEEE 58th Conference on Decision and Control (CDC)*, pages 2726–2731, December 2019. doi: 10.1109/CDC40024.2019.9029310. ISSN: 2576-2370.
- T. Gehr, M. Mirman, D. Drachler-Cohen, P. Tsankov, S. Chaudhuri, and M. Vechev. AI2: Safety and Robustness Certification of Neural Networks with Abstract Interpretation. In *2018 IEEE Symposium on Security and Privacy (SP)*, pages 3–18, May 2018. doi: 10.1109/SP.2018.00058.
- Ruobin Gong and Xiao-Li Meng. Judicious judgment meets unsettling updating: dilation, sure loss, and Simpson’s paradox. *Statistical Science*, 36(2):169–190, 2021.
- Chuan Guo, Geoff Pleiss, Yu Sun, and Kilian Q. Weinberger. On calibration of modern neural networks. In *Proceedings of the 34th International Conference on Machine Learning - Volume 70*, ICML'17, pages 1321–1330, Sydney, NSW, Australia, August 2017. JMLR.org.
- Chirag Gupta, Aleksandr Podkopaev, and Aaditya Ramdas. Distribution-free binary classification: prediction sets, confidence intervals and calibration. *arXiv:2006.10564 [cs, math, stat]*, February 2022. URL <http://arxiv.org/abs/2006.10564>. arXiv: 2006.10564.

- Peter J. Huber and Elvezio M. Ronchetti. *Robust statistics*. Wiley Series in Probability and Statistics. Hoboken, New Jersey : Wiley, 2nd edition, 2009.
- Radoslav Ivanov, Taylor Carpenter, James Weimer, Rajeev Alur, George Pappas, and Insup Lee. Verisig 2.0: Verification of Neural Network Controllers Using Taylor Model Preconditioning. In *Computer Aided Verification*, pages 249–262, Cham, 2021. Springer International Publishing. ISBN 978-3-030-81685-8.
- Radim Jiroušek and Prakash P. Shenoy. A new definition of entropy of belief functions in the Dempster–Shafer theory. *International Journal of Approximate Reasoning*, 92:49–65, 2018.
- Guy Katz, Clark Barrett, David Dill, Kyle Julian, and Mykel Kochenderfer. Reluplex: An Efficient SMT Solver for Verifying Deep Neural Networks. *arXiv:1702.01135 [cs]*, February 2017. URL <http://arxiv.org/abs/1702.01135>. arXiv: 1702.01135.
- Tobias Ladner and Matthias Althoff. Automatic Abstraction Refinement in Neural Network Verification using Sensitivity Analysis. In *Proceedings of the 26th ACM International Conference on Hybrid Systems: Computation and Control*, HSCC '23, pages 1–13, New York, NY, USA, May 2023. Association for Computing Machinery. ISBN 9798400700330. doi: 10.1145/3575870.3587129. URL <https://dl.acm.org/doi/10.1145/3575870.3587129>.
- Balaji Lakshminarayanan, Alexander Pritzel, and Charles Blundell. Simple and scalable predictive uncertainty estimation using deep ensembles. In *Proceedings of the 31st International Conference on Neural Information Processing Systems*, NIPS'17, pages 6405–6416, Red Hook, NY, USA, December 2017. Curran Associates Inc. ISBN 978-1-5108-6096-4.
- Kim G. Larsen and Axel Legay. Statistical Model Checking Past, Present, and Future. In Tiziana Margaria and Bernhard Steffen, editors, *Leveraging Applications of Formal Methods, Verification and Validation. Specialized Techniques and Applications*, Lecture Notes in Computer Science, pages 135–142, Berlin, Heidelberg, 2014. Springer. ISBN 978-3-662-45231-8. doi: 10.1007/978-3-662-45231-8\_10.
- Thomas Lew, Lucas Janson, Riccardo Bonalli, and Marco Pavone. A simple and efficient sampling-based algorithm for general reachability analysis. In Roya Firoozi, Negar Mehr, Esen Yel, Rika Antonova, Jeannette Bohg, Mac Schwager, and Mykel Kochenderfer, editors, *Proceedings of The 4th Annual Learning for Dynamics and Control Conference*, volume 168 of *Proceedings of Machine Learning Research*, pages 1086–1099. PMLR, 23–24 Jun 2022. URL <https://proceedings.mlr.press/v168/lew22a.html>.
- Haitao Liu, Yew-Soon Ong, Xiaobo Shen, and Jianfei Cai. When Gaussian Process Meets Big Data: A Review of Scalable GPs. *IEEE Transactions on Neural Networks and Learning Systems*, 31(11):4405–4423, November 2020. ISSN 2162-2388. doi: 10.1109/TNNLS.2019.2957109. Conference Name: IEEE Transactions on Neural Networks and Learning Systems.
- Rachel Luo, Shengjia Zhao, Jonathan Kuck, Boris Ivanovic, Silvio Savarese, Edward Schmerling, and Marco Pavone. Sample-efficient safety assurances using conformal prediction. In Steven M. LaValle, Jason M. O’Kane, Michael Otte, Dorsa Sadigh, and Pratap Tokekar, editors, *Algorithmic Foundations of Robotics XV*, pages 149–169, Cham, 2023. Springer International Publishing. ISBN 978-3-031-21090-7.

- Rhiannon Michelmore, Matthew Wicker, L. Laurenti, L. Cardelli, Y. Gal, and Marta Kwiatkowska. Uncertainty Quantification with Statistical Guarantees in End-to-End Autonomous Driving Control. *2020 IEEE International Conference on Robotics and Automation (ICRA)*, 2020. doi: 10.1109/ICRA40945.2020.9196844.
- Matthias Minderer, Josip Djolonga, Rob Romijnders, Frances Hubis, Xiaohua Zhai, Neil Houlsby, Dustin Tran, and Mario Lucic. Revisiting the Calibration of Modern Neural Networks. In *Advances in Neural Information Processing Systems*, volume 34, pages 15682–15694. Curran Associates, Inc., 2021.
- Sayan Mitra. *Verifying Cyber-Physical Systems: A Path to Safe Autonomy*. The MIT Press, Cambridge, Massachusetts, February 2021. ISBN 978-0-262-04480-6.
- Robert J. Moss, Mykel J. Kochenderfer, Maxime Gariel, and Arthur Dubois. Bayesian Safety Validation for Black-Box Systems. In *Conference proceedings of the 2023 AIAA AVIATION Forum*, May 2023. doi: 10.48550/arXiv.2305.02449. URL <http://arxiv.org/abs/2305.02449>. arXiv:2305.02449 [cs, stat].
- Anish Muthali, Haotian Shen, Sampada Deglurkar, Michael H. Lim, Rebecca Roelofs, Aleksandra Faust, and Claire Tomlin. Multi-agent reachability calibration with conformal prediction, 2023.
- Luis Oala, Cosmas Hei, Jan MacDonald, Maximilian Mrzt, Wojciech Samek, and Gitta Kutyniok. Interval neural networks: Uncertainty scores. *ArXiv*, abs/2003.11566, 2020.
- Harris Papadopoulos, Kostas Proedrou, Volodya Vovk, and Alex Gammerman. Inductive confidence machines for regression. In *Machine Learning: ECML 2002: 13th European Conference on Machine Learning Helsinki, Finland, August 19–23, 2002 Proceedings 13*, pages 345–356. Springer, 2002.
- Sangdon Park, Shuo Li, Osbert Bastani, and I. Lee. PAC Confidence Predictions for Deep Neural Network Classifiers. *ICLR*, 2021.
- Aleksandar Petrov, Carter Fang, Khang Minh Pham, You Hong Eng, James Guo Ming Fu, and Scott Drew Pendleton. HiddenGems: Efficient safety boundary detection with active learning. In *2022 IEEE/RSJ International Conference on Intelligent Robots and Systems (IROS)*, pages 5147–5154, October 2022. doi: 10.1109/IROS47612.2022.9982243. ISSN: 2153-0866.
- Xin Qin, Yuan Xian, Aditya Zutshi, Chuchu Fan, and Jyotirmoy Deshmukh. Statistical Verification of Autonomous Systems using Surrogate Models and Conformal Inference. In *Proc. of ICCPS’22*, July 2021. URL <http://arxiv.org/abs/2004.00279>. arXiv: 2004.00279.
- Xin Qin, Yuan Xia, Aditya Zutshi, Chuchu Fan, and Jyotirmoy V. Deshmukh. Statistical verification using surrogate models and conformal inference and a comparison with risk-aware verification. *ACM Trans. Cyber-Phys. Syst.*, dec 2023. ISSN 2378-962X. doi: 10.1145/3635160. URL <https://doi.org/10.1145/3635160>. Just Accepted.
- Carl Edward Rasmussen and Christopher K. I. Williams. *Gaussian Processes for Machine Learning*. The MIT Press, Cambridge, Mass, November 2005. ISBN 978-0-262-18253-9.

- Sanjit A. Seshia, Dorsa Sadigh, and S. Shankar Sastry. Toward verified artificial intelligence. *Communications of the ACM*, 65(7):46–55, June 2022. ISSN 0001-0782. doi: 10.1145/3503914. URL <https://dl.acm.org/doi/10.1145/3503914>.
- Glenn Shafer and Vladimir Vovk. A Tutorial on Conformal Prediction. *J. Mach. Learn. Res.*, 9: 371–421, June 2008. ISSN 1532-4435. URL <http://dl.acm.org/citation.cfm?id=1390681.1390693>.
- Chelsea Sidrane, Amir Maleki, Ahmed Irfan, and Mykel J. Kochenderfer. OVERT: an algorithm for safety verification of neural network control policies for nonlinear systems. *The Journal of Machine Learning Research*, 23(1):117:5090–117:5134, January 2022. ISSN 1532-4435.
- Rohan Sinha, Apoorva Sharma, Somrita Banerjee, Thomas Lew, Rachel Luo, Spencer M Richards, Yixiao Sun, Edward Schmerling, and Marco Pavone. A System-Level View on Out-of-Distribution Data in Robotics, 2022.
- Ralph C. Smith. *Uncertainty Quantification: Theory, Implementation, and Applications*. SIAM, December 2013. ISBN 978-1-61197-321-1. Google-Books-ID: 4c1GAgAAQBAJ.
- Jiayang Song, Deyun Lyu, Zhenya Zhang, Zhijie Wang, Tianyi Zhang, and Lei Ma. When Cyber-Physical Systems Meet AI: A Benchmark, an Evaluation, and a Way Forward. In *Proceedings of the 44th International Conference on Software Engineering: Software Engineering in Practice*, pages 343–352, May 2022. doi: 10.1145/3510457.3513049. URL <http://arxiv.org/abs/2111.04324>. arXiv:2111.04324 [cs].
- Sullivan. *Introduction to Uncertainty Quantification*. Springer, New York, NY, 1st ed. 2015 edition edition, December 2015. ISBN 978-3-319-23394-9.
- Hoang-Dung Tran, Xiaodong Yang, Diego Manzananas Lopez, Patrick Musau, Luan Viet Nguyen, Weiming Xiang, Stanley Bak, and Taylor T. Johnson. NNV: The Neural Network Verification Tool for Deep Neural Networks and Learning-Enabled Cyber-Physical Systems. In *Computer Aided Verification*, 2020.
- Matthias C.M. Troffaes and Gert de Cooman. *Lower Previsions*. Chichester, United Kingdom : John Wiley and Sons, 2014.
- Vladimir Vovk, Alex Gammerman, and Glenn Shafer. *Algorithmic Learning in a Random World*. Springer, New York, 2005 edition edition, March 2005. ISBN 978-0-387-00152-4.
- Peter Walley. *Statistical Reasoning with Imprecise Probabilities*, volume 42 of *Monographs on Statistics and Applied Probability*. London : Chapman and Hall, 1991.
- Yu Wang, Mojtaba Zarei, Borzoo Bonakdarpoor, and Miroslav Pajic. Probabilistic conformance for cyber-physical systems. In *Proceedings of the ACM/IEEE 12th International Conference on Cyber-Physical Systems, ICCPS '21*, pages 55–66, New York, NY, USA, May 2021. Association for Computing Machinery. ISBN 978-1-4503-8353-0. doi: 10.1145/3450267.3450534. URL <https://doi.org/10.1145/3450267.3450534>.
- Larry Wasserman. Recent methodological advances in robust Bayesian inference. *Bayesian statistics*, 4:483–502, 1992.



- Larry A. Wasserman and Joseph B. Kadane. Bayes' theorem for Choquet capacities. *The Annals of Statistics*, 18(3):1328–1339, 1990.
- Matthew Wicker, Luca Laurenti, Andrea Patane, and Marta Kwiatkowska. Probabilistic Safety for Bayesian Neural Networks. In *Proceedings of the 36th Conference on Uncertainty in Artificial Intelligence (UAI)*, pages 1198–1207. PMLR, August 2020. URL <https://proceedings.mlr.press/v124/wicker20a.html>. ISSN: 2640-3498.
- Mojtaba Zarei, Yu Wang, and Miroslav Pajic. Statistical verification of learning-based cyber-physical systems. In *Proceedings of the 23rd International Conference on Hybrid Systems: Computation and Control, HSCC '20*, pages 1–7, New York, NY, USA, April 2020. Association for Computing Machinery. ISBN 978-1-4503-7018-9. doi: 10.1145/3365365.3382209. URL <https://doi.org/10.1145/3365365.3382209>.
- Zhenya Zhang, Deyun Lyu, Paolo Arcaini, Lei Ma, Ichiro Hasuo, and Jianjun Zhao. FalsifAI: Falsification of AI-Enabled Hybrid Control Systems Guided by Time-Aware Coverage Criteria. *IEEE Transactions on Software Engineering*, 49(4):1842–1859, April 2023. ISSN 1939-3520. doi: 10.1109/TSE.2022.3194640. Conference Name: IEEE Transactions on Software Engineering.

## Appendix A. Appendix

### A.1. Proofs

**Proof** [Proof of Theorem 3] Let us write the partial derivative of  $\mathcal{L}(\underline{\Phi}, \bar{\Phi})$  with respect to  $\bar{\Phi}(x)$

$$\frac{\partial \mathcal{L}(\underline{\Phi}, \bar{\Phi})}{\partial \bar{\Phi}(x)} = \frac{\partial}{\partial \bar{\Phi}(x)} \sup_{P_X \in \mathcal{P}_X} \int_{\mathcal{X}} [\mathbb{E}_{Y|X}(\bar{m}^2) + \mathbb{E}_{Y|X}(\underline{m}^2) + \beta (\bar{\Phi}(x) - \underline{\Phi}(x))] P_X(\mathbf{d}x). \quad (4)$$

Since we assumed  $\mathcal{P}_X$  to be compact, then there is  $\tilde{P}_X \in \mathcal{P}_X$  such that

$$\begin{aligned} & \sup_{P_X \in \mathcal{P}_X} \int_{\mathcal{X}} [\mathbb{E}_{Y|X}(\bar{m}^2) + \mathbb{E}_{Y|X}(\underline{m}^2) + \beta (\bar{\Phi}(x) - \underline{\Phi}(x))] P_X(\mathbf{d}x) \\ &= \int_{\mathcal{X}} [\mathbb{E}_{Y|X}(\bar{m}^2) + \mathbb{E}_{Y|X}(\underline{m}^2) + \beta (\bar{\Phi}(x) - \underline{\Phi}(x))] \tilde{P}_X(\mathbf{d}x). \end{aligned}$$

Then, (4) can be rewritten as

$$\frac{\partial \mathcal{L}(\underline{\Phi}, \bar{\Phi})}{\partial \bar{\Phi}(x)} = \frac{\partial}{\partial \bar{\Phi}(x)} \int_{\mathcal{X}} [\mathbb{E}_{Y|X}(\bar{m}^2) + \mathbb{E}_{Y|X}(\underline{m}^2) + \beta (\bar{\Phi}(x) - \underline{\Phi}(x))] \tilde{P}_X(\mathbf{d}x).$$

From Leibniz integral rule and the additivity of the derivative operator, then, we can write

$$\begin{aligned} \frac{\partial \mathcal{L}(\underline{\Phi}, \bar{\Phi})}{\partial \bar{\Phi}(x)} &= \int_{\mathcal{X}} \frac{\partial}{\partial \bar{\Phi}(x)} [\mathbb{E}_{Y|X}(\bar{m}^2) + \mathbb{E}_{Y|X}(\underline{m}^2) + \beta (\bar{\Phi}(x) - \underline{\Phi}(x))] \tilde{P}_X(\mathbf{d}x) \\ &= \int_{\mathcal{X}} \frac{\partial}{\partial \bar{\Phi}(x)} \mathbb{E}_{Y|X}(\bar{m}^2) + \frac{\partial}{\partial \bar{\Phi}(x)} \mathbb{E}_{Y|X}(\underline{m}^2) + \frac{\partial}{\partial \bar{\Phi}(x)} [\beta (\bar{\Phi}(x) - \underline{\Phi}(x))] \tilde{P}_X(\mathbf{d}x). \end{aligned} \quad (5)$$

Since we assumed that  $\mathcal{P}_{Y|X}$  to be compact, there are  $P_{Y|X}^*$ ,  $P_{Y|X}^{**}$  in  $\mathcal{P}_{Y|X}$ , possibly different from each other, such that

$$\begin{aligned} \mathbb{E}_{Y|X}(\bar{m}^2) &:= \sup_{P_{Y|X} \in \mathcal{P}_{Y|X}} \int_{\mathcal{Y}} \max(y - \bar{\Phi}(x), 0)^2 P_{Y|X}(\mathbf{d}y) \\ &= \int_{\mathcal{Y}} \max(y - \bar{\Phi}(x), 0)^2 P_{Y|X}^*(\mathbf{d}y) =: \mathbb{E}_{Y|X}^*(\bar{m}^2) \end{aligned}$$

and

$$\begin{aligned} \mathbb{E}_{Y|X}(\underline{m}^2) &:= \sup_{P_{Y|X} \in \mathcal{P}_{Y|X}} \int_{\mathcal{Y}} \max(\underline{\Phi}(x) - y, 0)^2 P_{Y|X}(\mathbf{d}y) \\ &= \int_{\mathcal{Y}} \max(\underline{\Phi}(x) - y, 0)^2 P_{Y|X}^{**}(\mathbf{d}y) =: \mathbb{E}_{Y|X}^{**}(\underline{m}^2). \end{aligned}$$

So we can rewrite (5) as

$$\begin{aligned} \frac{\partial \mathcal{L}(\underline{\Phi}, \bar{\Phi})}{\partial \bar{\Phi}(x)} &= \int_{\mathcal{X}} \frac{\partial}{\partial \bar{\Phi}(x)} \mathbb{E}_{Y|X}^*(\bar{m}^2) + \frac{\partial}{\partial \bar{\Phi}(x)} \mathbb{E}_{Y|X}^{**}(\underline{m}^2) + \frac{\partial}{\partial \bar{\Phi}(x)} [\beta (\bar{\Phi}(x) - \underline{\Phi}(x))] \tilde{P}_X(\mathbf{d}x) \\ &= (-2) \int_{\mathcal{X}} \mathbb{E}_{Y|X}^*(\bar{m}) \tilde{P}_X(\mathbf{d}x) + \beta. \end{aligned} \quad (6)$$

Assuming that  $\mathcal{L}(\underline{\Phi}, \bar{\Phi})$  is optimized, we have that  $\partial \mathcal{L}(\underline{\Phi}, \bar{\Phi}) / \partial \bar{\Phi}(x) = 0$ , which by (6) holds if and only if

$$\frac{\beta}{2} = \int_{\mathcal{X}} \mathbb{E}_{Y|X}^*(\bar{m}) \tilde{P}_X(\mathbf{d}x) = \sup_{P_X \in \mathcal{P}_X} \int_{\mathcal{X}} \bar{\mathbb{E}}_{Y|X}(\bar{m}) P_X(\mathbf{d}x). \quad (7)$$

Analogously, we have that

$$\frac{\beta}{2} = \int_{\mathcal{X}} \mathbb{E}_{Y|X}^{**}(\underline{m}) \tilde{P}_X(\mathbf{d}x) = \sup_{P_X \in \mathcal{P}_X} \int_{\mathcal{X}} \bar{\mathbb{E}}_{Y|X}(\underline{m}) P_X(\mathbf{d}x). \quad (8)$$

Let now  $h_1(\zeta) := \max(\zeta - \bar{\Phi}(x), 0)$  and  $h_2(\zeta) := \max(\zeta + \underline{\Phi}(x), 0)$ . By Markov's inequality, we have that for all  $P_{Y|X} \in \mathcal{P}_{Y|X}$ ,

$$P_{Y|X}(y \geq \bar{\Phi}(x) + \lambda\beta) \leq \frac{\mathbb{E}_{Y|X}[h_1(y)]}{h_1(\bar{\Phi}(x) + \lambda\beta)} = \frac{\mathbb{E}_{Y|X}(\bar{m})}{\lambda\beta}.$$

This implies that

$$\bar{P}_{Y|X}(y \geq \bar{\Phi}(x) + \lambda\beta) \leq \frac{\bar{\mathbb{E}}_{Y|X}(\bar{m})}{\lambda\beta}. \quad (9)$$

Similarly,

$$\bar{P}_{Y|X}(y \leq \underline{\Phi}(x) - \lambda\beta) \leq \frac{\bar{\mathbb{E}}_{Y|X}(\underline{m})}{\lambda\beta}. \quad (10)$$

Recall that  $A = \{\underline{\Phi}(x) - \lambda\beta \leq y \leq \bar{\Phi}(x) + \lambda\beta\}$ ; then, we have the following

$$\mathbb{E}_X \left[ \underline{P}_{Y|X}(A) \right] = \mathbb{E}_X \left[ 1 - \bar{P}_{Y|X}(A^c) \right] \quad (11)$$

$$\begin{aligned} &= \inf_{P_X \in \mathcal{P}_X} \int_{\mathcal{X}} \left[ 1 - \bar{P}_{Y|X}(A^c) \right] P_X(\mathbf{d}x) \\ &= \inf_{P_X \in \mathcal{P}_X} \left[ 1 - \int_{\mathcal{X}} \bar{P}_{Y|X}(A^c) P_X(\mathbf{d}x) \right] \end{aligned} \quad (12)$$

$$\begin{aligned} &= 1 + \inf_{P_X \in \mathcal{P}_X} \left[ - \int_{\mathcal{X}} \bar{P}_{Y|X}(A^c) P_X(\mathbf{d}x) \right] \\ &= 1 - \sup_{P_X \in \mathcal{P}_X} \int_{\mathcal{X}} \bar{P}_{Y|X}(A^c) P_X(\mathbf{d}x) \\ &= 1 - \bar{\mathbb{E}}_X \left[ \bar{P}_{Y|X}(A^c) \right], \end{aligned} \quad (13)$$

where (11) comes from the conjugacy property of lower probabilities,  $\underline{P}(A) = 1 - \bar{P}(A^c)$ , (12) comes from the additivity property of an integral, and (13) is true because for a generic function  $f$ , we have that  $\sup -f = -\inf f$ . In turn, this chain of equalities implies that

$$\mathbb{E}_X \left[ \underline{P}_{Y|X}(A) \right] = 1 - \bar{\mathbb{E}}_X \left[ \bar{P}_{Y|X}(A^c) \right]. \quad (14)$$

Then, the following holds

$$\mathbb{E}_X[\underline{P}_{Y|X}(A)] = 1 - \overline{\mathbb{E}}_X[\overline{P}_{Y|X}(A^c)] \quad (15)$$

$$\begin{aligned} &= 1 - \sup_{P_X \in \mathcal{P}_X} \int_{\mathcal{X}} \sup_{P_{Y|X} \in \mathcal{P}_{Y|X}} [P_{Y|X}(y \leq \underline{\Phi}(x) - \lambda\beta) + P_{Y|X}(y \geq \overline{\Phi}(x) + \lambda\beta)] P_X(\mathrm{d}x) \\ &\geq 1 - \sup_{P_X \in \mathcal{P}_X} \int_{\mathcal{X}} \overline{P}_{Y|X}(y \leq \underline{\Phi}(x) - \lambda\beta) P_X(\mathrm{d}x) - \sup_{P_X \in \mathcal{P}_X} \int_{\mathcal{X}} \overline{P}_{Y|X}(y \geq \overline{\Phi}(x) + \lambda\beta) P_X(\mathrm{d}x) \end{aligned} \quad (16)$$

$$\geq 1 - \frac{1}{\lambda\beta} \left[ \sup_{P_X \in \mathcal{P}_X} \int_{\mathcal{X}} \overline{\mathbb{E}}_{Y|X}(\overline{m}) P_X(\mathrm{d}x) + \sup_{P_X \in \mathcal{P}_X} \int_{\mathcal{X}} \overline{\mathbb{E}}_{Y|X}(m) P_X(\mathrm{d}x) \right] \quad (17)$$

$$= 1 - \frac{1}{\lambda\beta} \left[ \frac{\beta}{2} + \frac{\beta}{2} \right] \quad (18)$$

$$= 1 - \frac{1}{\lambda}.$$

Equality (15) comes from (14). Inequality (16) comes from well-known properties of the sup operator. Inequality (17) comes from (9) and (10). Finally, equality (18) comes from (7) and (8). ■

**Proof** [Proof of Corollary 4] By Theorem 3 we have that  $\mathbb{E}_X[\underline{P}_{Y|X}(A)] \geq 1 - 1/\lambda$ . In addition, by the properties of regular probabilities and upper probabilities, we have that  $\overline{\mathbb{E}}_X[\overline{P}_{Y|X}(A)] \leq 1$ . This implies immediately that  $\overline{\mathbb{E}}_X[\overline{P}_{Y|X}(A)] - \mathbb{E}_X[\underline{P}_{Y|X}(A)] \leq 1/\lambda$ . ■

**Proof** [Proof of Corollary 5] We have that

$$\begin{aligned} \frac{1}{\lambda} &\geq \overline{\mathbb{E}}_X[\overline{P}_{Y|X}(y < \underline{\Phi}(x) - \lambda\beta, y > \overline{\Phi}(x) + \lambda\beta)] \\ &= \sup_{P_X \in \mathcal{P}_X} \int_{\mathcal{X}} \sup_{P_{Y|X} \in \mathcal{P}_{Y|X}} P_{Y|X}(y < \underline{\Phi}(x) - \lambda\beta, y > \overline{\Phi}(x) + \lambda\beta) P_X(\mathrm{d}x), \end{aligned} \quad (19)$$

where inequality (19) comes from Theorem 3. Now, by our assumption that both  $\mathcal{P}_X$  and  $\mathcal{P}_{Y|X}$  are compact, there exist  $\tilde{P}_X \in \mathcal{P}_X$  and  $P_{Y|X}^* \in \mathcal{P}_{Y|X}$  such that

$$\begin{aligned} &\sup_{P_X \in \mathcal{P}_X} \int_{\mathcal{X}} \sup_{P_{Y|X} \in \mathcal{P}_{Y|X}} P_{Y|X}(y < \underline{\Phi}(x) - \lambda\beta, y > \overline{\Phi}(x) + \lambda\beta) P_X(\mathrm{d}x) \\ &= \int_{\mathcal{X}} P_{Y|X}^*(y < \underline{\Phi}(x) - \lambda\beta, y > \overline{\Phi}(x) + \lambda\beta) \tilde{P}_X(\mathrm{d}x). \end{aligned}$$

In addition, it follows immediately that

$$\begin{aligned} &\int_{\mathcal{X}} P_{Y|X}^*(y < \underline{\Phi}(x) - \lambda\beta, y > \overline{\Phi}(x) + \lambda\beta) \tilde{P}_X(\mathrm{d}x) \\ &\geq \int_{\mathcal{X}} \alpha \mathbf{1} \left\{ P_{Y|X}^*(y < \underline{\Phi}(x) - \lambda\beta, y > \overline{\Phi}(x) + \lambda\beta) > \alpha \right\} \tilde{P}_X(\mathrm{d}x) \\ &= \sup_{P_X \in \mathcal{P}_X} \int_{\mathcal{X}} \alpha \mathbf{1} \left\{ \sup_{P_{Y|X} \in \mathcal{P}_{Y|X}} P_{Y|X}(y < \underline{\Phi}(x) - \lambda\beta, y > \overline{\Phi}(x) + \lambda\beta) > \alpha \right\} \tilde{P}_X(\mathrm{d}x) \\ &= \overline{\mathbb{E}}_X[\alpha \mathbf{1} \{ \overline{P}_{Y|X}(y < \underline{\Phi}(x) - \lambda\beta, y > \overline{\Phi}(x) + \lambda\beta) > \alpha \}]. \end{aligned}$$

By (19), this implies in turn that

$$\frac{1}{\lambda} \geq \bar{E}_X [\alpha \mathbf{1} \{ \bar{P}_{Y|X} (y < \underline{\Phi}(x) - \lambda\beta, y > \bar{\Phi}(x) + \lambda\beta) > \alpha \} ],$$

which holds if and only if

$$\frac{1}{\lambda\alpha} \geq \bar{E}_X [\mathbf{1} \{ \bar{P}_{Y|X} (y < \underline{\Phi}(x) - \lambda\beta, y > \bar{\Phi}(x) + \lambda\beta) > \alpha \} ],$$

concluding the proof. ■

## Appendix B. Additional Experimental Results

**Implementation Details** The control policies were trained using the Deep Deterministic Policy Gradient algorithm of  $10^7$  time steps, with a learning rate of  $3 \times 10^{-4}$ , and a buffer size of  $10^7$ . We used a 2-layer feedforward neural network with ReLU activation layers and a width of 256. The uncertainty maximization step in Algorithm 1 was performed with a timeout of  $5 \times 10^3$  seconds, on a 96-core Intel Xeon Processor running at 3 GHz, and 800 GB RAM.

**Additional Experimental Results** We present additional results here. Table 4 and Table 5 summarize the coverage results of INN and CP in the in-distribution case. Additionally, Table 6, and Table 7 summarize the results when samples are drawn from a uniform distribution. This latter case, as we reiterate, is an out-of-distribution setting for CP, but is a within family distribution for INNs. As we observe that in some cases while CP fails provide coverage under 95%, INNs are observed to have much better coverage. However, this comes at the cost of slightly higher interval widths.

Environment	$\mathcal{X}$ Dim	Conformal Prediction		INN (ours)	
		Coverage (%)	Interval Size	Coverage (%)	Interval Size
Ant	29	97	4.1	99	4.4
Half-Cheetah	18	94	$4.9 \times 10^{-1}$	100	3.3
Hopper	12	95	1.6	100	2.5
Humanoid	47	93	1.8	99	3.1
Humanoid-Standup	47	97	158	99	248
Inverted Double Pendulum	6	95	$6.8 \times 10^{-3}$	100	$4.1 \times 10^{-1}$
Inverted Pendulum	4	95	$1.3 \times 10^{-4}$	100	$4.5 \times 10^{-1}$
Reacher	8	96	$4.8 \times 10^{-2}$	100	$4.3 \times 10^{-1}$
Swimmer	10	95	$4 \times 10^{-3}$	100	$4.1 \times 10^{-1}$
Walker2d	18	95	6	99	6.1

Table 4: We compare the coverage rates and size of prediction regions between an INN and CP for  $\beta = 10^{-2}$  when the test samples are in-distribution.  $\mathcal{X}$  denotes the input space. The interval size of the INN is an average value across the samples.

Environment	$\mathcal{X}$ Dim	Conformal Prediction		INN (ours)	
		Coverage (%)	Interval Size	Coverage (%)	Interval Size
Ant	29	95	3.9	99	4.3
Half-Cheetah	18	96	$5.1 \times 10^{-1}$	99	4
Hopper	12	95	2.5	99	2.4
Humanoid	47	95	2.34	99.5	2.89
Humanoid-Standup	47	94	138	99	258
Inverted Double Pendulum	6	96	$7 \times 10^{-3}$	100	3.55
Inverted Pendulum	4	97	$2 \times 10^{-4}$	100	$6.2 \times 10^{-1}$
Reacher	8	95	$4.3 \times 10^{-2}$	100	$4.8 \times 10^{-2}$
Swimmer	10	94	$2.9 \times 10^{-3}$	100	$9 \times 10^{-2}$
Walker2d	18	96	5.55	99	5.34

Table 5: We compare the coverage rates and size of prediction regions between an INN and CP for  $\beta = 10^{-4}$  when the test samples are in-distribution.  $\mathcal{X}$  denotes the input space. The interval size of the INN is an average value across the samples.

Environment	$\mathcal{X}$ Dim	Conformal Prediction		INN (ours)	
		Coverage (%)	Interval Size	Coverage (%)	Interval Size
Ant	29	97	4.1	100	4.6
Half-Cheetah	18	95	$5.0 \times 10^{-1}$	100	1.56
Hopper	12	90	1.6	100	2.8
Humanoid	47	92	1.8	100	3.3
Humanoid-Standup	47	96	158	99	240
Inverted Double Pendulum	6	95	$6.8 \times 10^{-3}$	100	$4.1 \times 10^{-1}$
Inverted Pendulum	4	99	$1.3 \times 10^{-4}$	100	$4.5 \times 10^{-1}$
Reacher	8	98	$4.9 \times 10^{-2}$	100	$4.4 \times 10^{-1}$
Swimmer	10	96	$4.4 \times 10^{-3}$	100	$4.1 \times 10^{-1}$
Walker2d	18	99	6	98	5.2

Table 6: We compare the coverage rates and size of prediction regions between an INN and CP for  $\beta = 10^{-2}$  when the test samples are out-of-distribution.  $\mathcal{X}$  denotes the input space. The interval size of the INN is an average value across the samples.

### B.1. Execution Time

Timings of the uncertainty sampling step, dependence on the set size, and training multiple DNNs. The costs of collecting samples are identical for the case of conformal prediction (CP) and INNs. However, the main difference is in the uncertainty maximization step (Algorithm 1) which uses a DNN verifier. We collected the execution time for the setting of  $\delta = 0.05$  in the paper, and report these in Table 8. We additionally report it for a larger  $\delta = 0.07$  as well. We observe that the NN verifier was able to complete within reasonable times for most of the benchmarks. As expected it generally takes longer for a larger search interval. However, note that these are in design time. At runtime the monitor is just executing 3, 2 layer NNs with 50 ReLU neurons in each layer.

Environment	$\mathcal{X}$ Dim	Conformal Prediction		INN (ours)	
		Coverage (%)	Interval Size	Coverage (%)	Interval Size
Ant	29	97	3.9	100	4.3
Half-Cheetah	18	96	$5.2 \times 10^{-1}$	100	4.5
Hopper	12	95	2.5	100	2.5
Humanoid	47	96	2.3	100	2.93
Humanoid-Standup	47	95	137	100	263
Inverted Double Pendulum	6	96	$7.1 \times 10^{-3}$	100	3.6
Inverted Pendulum	4	98	$2.3 \times 10^{-4}$	100	$6.2 \times 10^{-1}$
Reacher	8	98	$4.9 \times 10^{-2}$	100	$4.4 \times 10^{-1}$
Swimmer	10	96	$4.4 \times 10^{-3}$	100	$4.1 \times 10^{-1}$
Walker2d	18	94	5.5	100	5.5

Table 7: We compare the coverage rates and size of prediction regions between an INN and CP for  $\beta = 10^{-4}$  when the test samples are out-of-distribution.  $\mathcal{X}$  denotes the input space. The interval size of the INN is an average value across the samples.

Environment	$\mathcal{X}$ Dim	$\delta = 0.05$	$\delta = 0.07$
		Mean & Std	Mean & Std
Ant	29	$127 \pm 199$	$184 \pm 289$
Half-Cheetah	18	$10 \pm 3$	$13 \pm 7$
Hopper	12	$15 \pm 13$	$6 \pm 3$
Humanoid	47	$31 \pm 11$	$149 \pm 209$
Humanoid-Standup	47	$20 \pm 5$	$51 \pm 46$
Inverted Double Pend.	6	$2.4 \pm 1$	$2.5 \pm 1$
Inverted Pendulum	4	$1.3 \pm 0.3$	$1.5 \pm 0.3$
Reacher	8	$9 \pm 3.7$	$40 \pm 46$
Swimmer	10	$5 \pm 1.4$	$6 \pm 2.6$
Walker2d	18	$8.5 \pm 3.8$	$11.6 \pm 5.1$

Table 8: Time in seconds for uncertainty maximization